International Journal of Mechanical and Production Engineering, ISSN(p): 2320-2092, ISSN(e): 2321-2071
Volume- 6, Issue-4, Apr.-2018, http://iraj.in

CRASH SIMULATION OF A PIECEWISELY-INTEGRATED COMPOSITEBUMPER BEAMS

[1]CHAN HEE JEONG, [2]HYUN SEOK OH, [3]SEOK WOO HAM, [1]GYEONG SEOK KIM, [5]SEUNGNEO SON, [6]YUNG SUNG CHO, [7]SEONG S. CHEON

[1,2,3,4,7]Kongju Nat'l University, [5,6]ITS Korea
E-mail: [1]chj4944@kongju.ac.kr, [2]hsoh2403@kongju.ac.kr, [3]wooya@kongju.ac.kr, [4]gskim23@kongju.ac.kr, [5]snson@itskorea.kr, [6]standard@itskorea.kr, [7]sscheon@kongju.ac.kr

Abstract - The aim of the current work is to characterise a piecewisely-integrated composite bumper beam against the IIHS bumper crash protocol, therefore, IIHS bumper crash FE analysis for an aluminium type bumper beam was carried out to get the information about the dominant loading types at several regions in the bumper beam during crash. In the meantime, robust stacking sequences against tension and compression have been searched for using FE analysis of a coupon type model. After determining most effective stacking sequences for tension and compression, three-point bending simulation was preliminarily carried out to investigate the combination performance of tension dominant and compression dominant stacking sequences. Finally, IIHS bumper crash FE analysis for the piecewisely integrated composite bumper beam was conducted and the result was compared with other types of composite bumper beams. It was found that the newly suggested piecewisely-integrated composite bumper beam showed superior crashworthy behaviour to those of uni-modal stacking sequence composite bumper beams.

Index Terms - Bumper beam, IIHS crash, piecewisely integrated composite (PIC), stacking sequence

I. INTRODUCTION

Crashworthiness and lightweight characteristics of automotive vehicle structures are crucial targets in coachwork nowadays because of rigorously renewed vehicle safety regulations, high demanding of energy savings as well as reducing the emission of carbon dioxide, therefore, materials of automotive parts have been gradually switched from conventional ferrous metals to high strength steels, aluminium, plastics, composites and porous structures. Specifically, composites have excellent material properties such as specific stiffness and specific strength compared to metals and other traditional materials, therefore, they are attracting various fields of industries for their extensive applications. Of particular interest to this study is the use of composites in automotive bumper beams to promote the lightweight effect and crashworthiness simultaneously.

Automotive bumper beams have a key role to protect passengers from being attacked by sudden external crashes. Also, bumper beams, together with other automotive structures such as front side members, cross members and fender apron, absorb external crash energy effectively. On the other hand, contribution of bumper beam is maximized when vehicles are undergoing a low velocity crash case. One of representative low-velocity cases is IIHS (Insurance institute for highway safety) barrier crash, which is known that a car of 15 km/h moves toward a convex shaped barrier. Therefore, each part of the automotive bumper beam is experiencing different types of loading owing to the convex shaped IIHS barrier which contains honeycomb structures of uneven distribution of stiffness. It is necessary to figure out the dominant loading type and direction at every region in the bumper beam to correspondingly design the individual fibre orientation.

Cheon et al [1] suggested a novel type hybrid composite bumper beam for passenger cars and performed FE analysis and crash test. Hosseinzadeh et al [2] carried out parametric studies for designing composite bumper beams against low velocity impact. Davoodi et al. [3,4] measured mechanical properties of bio-composite and concept design of passenger car bumper beams. Belingardi et al. [5] optimized pultruded composite bumper beam profile by numerical simulation. Kim et al. [6] also optimised automotive hybrid composite bumper beam. As far as concerned, previous researches normally applied the monotonic stacking sequence to entire body of composite bumper beam without changing. The aim of the current work is to check the eligibility of a piecewisely-integrated composite (PIC) bumper beam with characterisation against the IIHS (Insurance institute for highway safety) bumper crash protocol [7]. Therefore, IIHS bumper crash FE analysis for an aluminium type bumper beam was carried out to get the information about the dominant loading types at several regions in the bumper beam during crash. In the meantime, robust stacking sequences against tension and compression have been searched for using FE analysis of a coupon type model. After determining most effective stacking sequences for tension and compression, three-point bending simulation was preliminarily carried out to investigate the combination performance of tension dominant and compression dominant stacking sequences. Finally, IIHS bumper crash FE analysis for the PIC bumper beam was conducted and the result was

compared with other types of composite bumper beams.

II. IIHS BUMPER CRASH AND LOADING TYPES

Insurance institute for highway safety suggested bumper test [7] at 10 km/h with a convex shape wall to investigate the failure behaviour of automotive bumpers. In the present study, IIHS bumper crash FE analysis for an existing aluminium bumper beam was carried out using LS-DYNA to get the information about the dominant loading type at several regions in the bumper beam during crash. Fig. 1 illustrated the FE model for IIHS bumper crash analysis for an aluminium bumper beam with IIHS barrier. 2,000 kg average weight of passenger car and the center of gravity location with proper mass moments of inertia along with axes of a vehicle were considered in the model without vehicle FE model for the sake of computational economy.

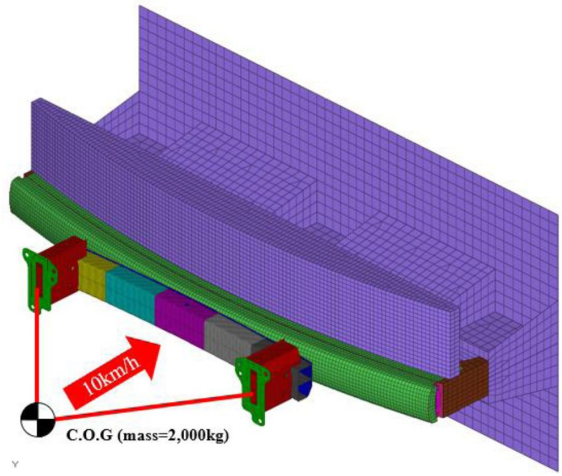

Fig. 1. IIHS bumper crash analysis (Full overlap).

The cross-section of the bumper beam, which was borrowed from an existing vehicle, consists of rectangular with horizontal rib as shown below.

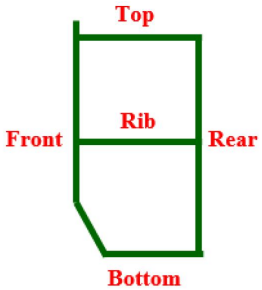

Fig. 2. The cross-section of the bumper beam.

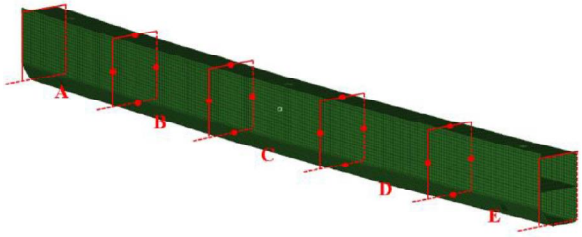

Fig. 3. Five regions of bumper beam.

Also, the bumper beam was divided into five regions in the longitudinal direction, i.e. A, B, C, D and E regions from the right to left as shown in Fig. 3 to investigate the loading type in the each region with the help of triaxiality [8].

The triaxiality is defined by Eqn (1).

$$\eta = \frac{\sigma_m}{\bar{\sigma}} \tag{1}$$

where,

$$\sigma_m = \frac{1}{3}(\sigma_1 + \sigma_2 + \sigma_3) \tag{2}$$

and

$$\bar{\sigma} = \sqrt{\frac{1}{2}[(\sigma_1 - \sigma_2)^2 + (\sigma_2 - \sigma_3)^2 + (\sigma_3 - \sigma_1)^2]} \tag{3}$$

Also, σ_1, σ_2 and σ_3 are representing principal stresses along with each direction.

Triaxiality is positive when the resultant loading is catagorised as tension, on the other hand, it is negative if the loading is compressive.

Triaxiality of each region was calculated and the results were summarised in Table I.

Table I. Signs of triaxiality of each region

	A	B	C	D	E
Front	-	-	-	-	-
Rear	+	+	+	+	+
Top	+	-	+	-	+
Bottom	-	-	+	-	-
Rib	-	-	-	-	-

It was found that the aluminium bumper beam was undergoing different types of external loading depending upon the location of bumper beam during IIHS crash.

III. EFFECTIVE STACKING SEQUENCES FOR TENSION AND COMPRESSION

Five representative stacking sequences [9,10] were considered, i.e., $[\pm 45/90/0_2]_{3S}$, $[\pm 5/\pm 45/90]_{3S}$, $[0_2/90/\pm 45]_{3S}$, $[\pm 45/\bar{0}]_{6S}$ and $[90/0/\bar{0}]_{6S}$. Tensile and compressive analyses were performed for composite coupon specimen and first ply failure loads were observed based on the Tsai-Wu failure criterion using S-glass epoxy composite material [11]. Fig. 4. showed examples for the tensile and the compressive FE analyses.

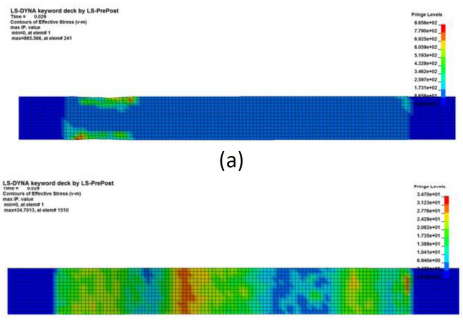

(a)

(b)

Fig. 4. Composite coupon simulation: (a) Tension, (b) compression.

Tables II and III indicated the coupon analysis results.

Table II. Tension analysis for composite coupon

Stacking sequence	First ply failure load (kN)	Absorbed energy (kJ)
$[\pm 45/90/0_2]_{3S}$	32.2	2.53
$[\pm 5/\pm 45/90]_{3S}$	27.5	1.60
$[0_2/90/\pm 45]_{3S}$	10.0	1.01
$[\pm 45/\bar{0}]_{6S}$	34.1	3.17
$[90/0/\bar{0}]_{6S}$	31.9	1.84

Table III. Compression analysis for composite coupon

Stacking sequence	First ply failure load (kN)	Absorbed energy (kJ)
$[\pm 45/90/0_2]_{3S}$	13.9	2.30
$[\pm 5/\pm 45/90]_{3S}$	9.6	1.88
$[0_2/90/\pm 45]_{3S}$	10.1	2.05
$[\pm 45/\bar{0}]_{6S}$	14.1	2.36
$[90/0/\bar{0}]_{6S}$	33.1	2.45

From the maximum values of first ply failure loading as well as absorbed energy characteristics, $[\pm 45/\bar{0}]_{6S}$ was selected for tension dominant stacking sequence, and $[90/0/\bar{0}]_{6S}$ was chosen for compression.

IV. THREE POINT BENDING ANALYSIS

Three-point bending simulation was preliminarily carried out to investigate the combination performance of tension dominant and compression dominant stacking sequences. Fig. 5 showed the FE model of three-point bending analysis.

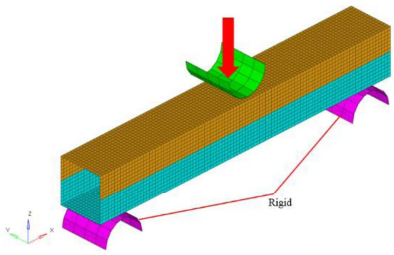

Fig. 5. FE model for three-point bending analysis.

Stacking sequences for the upper part and the lower part of the PIC model were $[90/0/\bar{0}]_{6S}$ and $[\pm 45/\bar{0}]_{6S}$, respectively.

Also, composites with uni-modal stacking sequences were simulated and compared their results as shown in Table IV.

Table IV. Compression analysis for composite coupon

Stacking sequence	First ply failure load (kN)	Absorbed energy (kJ)
$[\pm 45/90/0_2]_{3S}$	7.10	170.4
$[\pm 5/\pm 45/90]_{3S}$	6.37	181.1
$[0_2/90/\pm 45]_{3S}$	6.44	180.9
$[\pm 45/\bar{0}]_{6S}$	6.96	181.3
$[90/0/\bar{0}]_{6S}$	6.37	191.4
PIC	7.84	210.0

It was revealed that the PIC model showed superior bending characteristics compared to other composites with uni-modal stacking sequences.

V. IIHS BUMPER CRASH ANALYSIS FOR COMPOSITE BUMPER BEAMS

The PIC bumper beam was modeled with tension dominant stacking sequence ($[\pm 45/\bar{0}]_{6S}$) and compression dominant stacking sequence ($[90/0/\bar{0}]_{6S}$) based on the Table I and IIHS bumper crash FE analysis for the PIC bumper beam was conducted and the result was compared with other types of composite bumper beams from the maximum deformation and the lowest failure index of Tsai-Wu criterion. Table V summarised the IIHS bumper crash analyses and Fig. 6 showed the curve of external load associated with time and deformation. Deformation in Table V was measured by the horizontal length change of rib in the centre position of longitudinal direction.

Table V. IIHS bumper crash analysis results

Stacking sequence	Deformation (mm)	Max failure index
$[\pm 45/90/0_2]_{3S}$	8.15	21.89
$[\pm 5/\pm 45/90]_{3S}$	9.41	17.03
$[0_2/90/\pm 45]_{3S}$	7.94	9.55
$[\pm 45/\bar{0}]_{6S}$	8.54	3.12
$[90/0/\bar{0}]_{6S}$	9.22	3.01
PIC	7.74	1.67

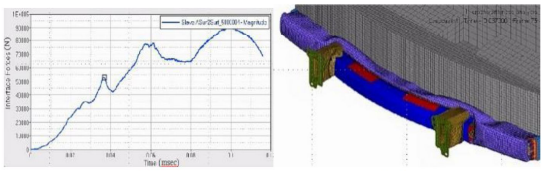

(a) (b)

Fig. 6. IIHS bumper simulation: (a) External force vs. time curve, (b) deformation of PIC bumper beam.

It was also unveiled that the PIC bumper beam is competitive compared with composite bumper beam with uni-modal stacking sequences.

CONCLUSION

IIHS bumper crash analysis for the PIC bumper beam was conducted and the results were compared with composite bumper beams with uni-modal stacking sequences. The stacking sequence $[\pm 45/\bar{0}]_{6S}$ was found to be the most effective during tensile loading, on the other hand, $[90/0/\bar{0}]_{6S}$ for compressive loading. The PIC bumper beam showed superior characteristics both for three-point bending and IIHS bumper crash. By the way, the tension dominant regions and compression dominant regions of the bumper beam during IIHS crash is desirable to be re-investigated instead of uniform length of five regions for calculating triaxiality in the future.

ACKNOWLEDGEMENT

This research was supported by a grant (17TLRP-B103927-03) from Transportation logistics research Program funded by Ministry of Land, Infrastructure and Transport of Korean government.

REFERENCES

[1] S. S. Cheon, J. H. Choi and D. G. Lee, "Development of the composite bumper beam for passenger cars," Composite Structures, vol. 32, pp. 491-499, 1995.

[2] R. Hosseinzadeh, M. M. Shokrieh, and L. B. Lessard, "Parametric study of automotive composite bumper beams subjected to low-velocity impacts," Composite Structures, vol. 68, pp. 419-427, May 2005.

[3] M. M. Davoodi, S. M. Sapuan, D. Ahmad, A. Ali, A. Khalina and M. Jonoobi, "Mechanical properties of hybrid kenaf/glass reinforced epoxy composite for passenger car bumper beam," Materials & Design, vol. 31, pp. 4927-4932, December 2010.

[4] M. M. Davoodi, S. M. Sapuan, D. Ahmad, A. Aidy, A. Khalina and M. Jonoobi, "Concept selection of car bumper beam with developed hybrid bio-composite material," Materials & Design, vol. 32, pp. 4857-4865, December 2011.

[5] G. Belingardi, A. T. Beyene and E. G. Koricho, "Geometrical optimization of bumper beam profile made of pultruded composite by numerical simulation," Composite Structures, vol. 102, pp. 217-225, August 2013.

[6] D. H. Kim, H. G. Kim and H. S. Kim, "Design optimization and manufacture of hybrid glass/carbon fiber reinforced composite bumper beam for automobile vehicle," Composite Structures, vol. 131, pp. 742-752, Nov. 2015.

[7] Bumper test protocol (Version VI), Insurance institute for highway safety, April 2007.

[8] Y. Bai, X. Teng and T. Wierzbicki, "On the application of stress triaxiality formula for plane strain fracture testing," J. Engineering Materials & Technology, Trans. ASME, Vol 131, 021002, April 2009.

[9] S. S. Cheon, D. G. Lee and K. S. Jeong," Composite side-door impact beams for passenger cars," Composite Structures, Vol. 38, pp. 229-239, 1997.

[10] G. Allaire and G. Delgado, "Stacking sequence and shape optimization of laminated composite plates via a level-set method," J. the Mechanics and Physics of Solids, Vol. 97, pp. 168-196, December 2016.

[11] D. G. Lee and N. P. Suh, Axiomatic design and fabrication of composite structures, Oxford University Press, New York, 2006.

★★★